Infrared Physics & Technology 64 (2014) 62–65

Contents lists available at ScienceDirect

Infrared Physics & Technology

journal homepage: www.elsevier.com/locate/infrared

# Cooled P-InAsSbP/n-InAs/N-InAsSbP double heterostructure photodiodes

P.N. Brunkov, N.D. Il'inskaya, S.A. Karandashev, A.A. Lavrov, B.A. Matveev *, M.A. Remennyi, N.M. Stus', A.A. Usikova

*Ioffe Physical-Technical Institute of the Russian Academy of Sciences, 26 Polytekhnicheskaya, St. Petersburg 194021, Russian Federation*

## HIGHLIGHTS

- We tested for the first time InAs double heterostructure photodiodes at low temperatures.
- InAs DH photodiodes exhibited superior performance compared to any InAs bulk diode.
- InAs DH heterostructures promise new trends in photodiode fabrication.

## ARTICLE INFO

*Article history:*
Received 6 November 2013
Available online 18 February 2014

*Keywords:*
Dark current
Photodiode structures
IR sensors

## ABSTRACT

Double heterostructure (DH) photodiodes (PDs) with InAs active layer and back-side illumination have been studied in the 100–300 K temperature range. Temperature dependence of a spectral response was standard for InAs based PDs while saturation current (or zero bias resistance) was characterized by a single value of the activation energy with domination of a diffusion current at most temperatures. As a result the simulated detectivity value was beyond the known numbers for homo- and heterojunction InAs PDs.



## 1. Introduction

For a number of years Mercury Cadmium Telluride (MCT) was main semiconductor material of IR photoelectronics [1], however $A^3B^5$ materials offer better metallurgical stability and tolerance to moisture and thus one can find now numerous groups writing acknowledgments for funding scientific research on $A^3B^5$ heterostructure photodiodes (PDs). PDs with active regions made from InAs(Sb) operate in the first atmospheric window (3–5 μm) and have a variety of applications including pyrometry [2], gas analysis [3] and thermovoltaic energy generation [4,5]. There is a number of theoretical and experimental papers devoted to bulk InAs [6] and heterostructure PDs including single (SH) [4,5,7–13] and double heterostructure (DH) [8] PDs with P-$InAs_{1-x-y}Sb_xP_y$ claddings lattice matched to InAs ($y = 2.2x$). InAs based heterostructure PDs exhibited superior performance in terms of detectivity ($D^*$) and zero bias resistance ($R_o$) values at ambient [8,10] and low temperatures [12] and several companies have already introduced these PDs in their product lists. Moreover p-InAsSbP/n-InAs based diodes with broad reflective anode contact offer "vertical" lasing at 77 K [14] and above unity wall plug efficiency due to thermo-electric pumping at room temperature [15]. On the other hand there is still a room for improvements as surface leakage [6], high dark current [11] and low breakdown voltage [12] are still among disadvantages of the existing PDs. InAs DH PDs offer enhanced zero bias resistance (value of merit for PDs) at ambient temperature evidently due to the presence of additional n-InAs/N-InAsSbP heterojunction [16], however to the best of our knowledge there has been only one paper describing InAs DH PD performance limited to ambient and elevated temperatures only [8] and no attempts have been undertaken so far to study P-InAsSbP/n-InAs/N-InAsSbP DH PDs at low temperatures and medium cooling.

We present data and analysis of the dark current and spectral response of P-InAsSbP/n-InAs/N-InAsSbP DH PDs at room temperature and medium cooling (in the 100–300 K temperature range).

## 2. Device fabrication and measurements

DHs were similar to those described in [8] and consisted of 90 μm thick heavily doped $n^+$-InAs (Sn) (100) substrates with an electron concentration of $n^+ = (2–3) \times 10^{18}$ $cm^{-3}$ and three epilayers lattice matched with the substrate. They represented 2–3 μm

* Corresponding author. Tel.: +7 8122927955; fax: +7 8122971017.
*E-mail addresses:* bmat@iropt3.ioffe.ru, ioffeled@mail.ru (B.A. Matveev).

http://dx.doi.org/10.1016/j.infrared.2014.01.010
1350-4495/

thick wide-gap N-$InAs_{1-x-y}Sb_xP_y$ ($y \approx 0.18$) confining layer, 4–6 μm thick n-InAs active region and 2–3 μm thick wide-gap P-$InAs_{1-x-y}Sb_xP_y$ (Zn) ($y \approx 0.18$, $P = (2–5) \times 10^{17}$ $cm^{-3}$) cap layer (see Fig. 1a where energy gap discontinuities constituted to $\Delta E_c = 120$ meV and $\Delta E_v = -30$ meV (300 K) [16] in accordance with formalism and band gap parameters suggested in [17]). There is curtain ground for suggesting coincidence (within the experimental accuracy) of p–n junction position and heterointerface as presented in Fig. 1a – indeed the AFM measurements disclosed in [13] confirm that the displacement of the p–n junction position and InAsSbP(Zn)/InAs interface was less than 0.3 μm in p-InAsSbP/$n^0$-InAs/$n^+$-InAs single heterostructures grown in a very similar to samples under discussion manner. Nearly the same results on p–n junction displacement have been recently obtained in the DH samples and this data will be published shortly. The above displacement is negligible compared to 5–10 μm in close structures described by other authors (see e.g. [11]) and is a distinguishing feature of the samples in the present study.

The heterostructures were processed by IoffeLED, Ltd. company using standard photolithography and wet etching processes into rectangular chips with mesa as high as 15–20 μm (see Fig. 1b) and ~(200 × 200) μm square p–n junction area. 150 × 150 μm square reflective Cr–Au–Ni–Au anode ($R \sim 0.6$) onto a P-InAsSbP epilayer and cathode placed on the same wafer side outside mesa provided connection of the heterostructure to external circuits. PD chips were mounted onto PD34Sr or TO-18 cases that allow backside illumination (BSI) mode of operation, that is, penetration of photons through a transparent $n^+$-InAs substrate without shadowing by electrical contacts (see horizontal arrow in Fig. 1a). Some of the PDs contained Si immersion lens attached to the $n^+$-InAs surface by a chalcogenide glue as described elsewhere [8,10]. The

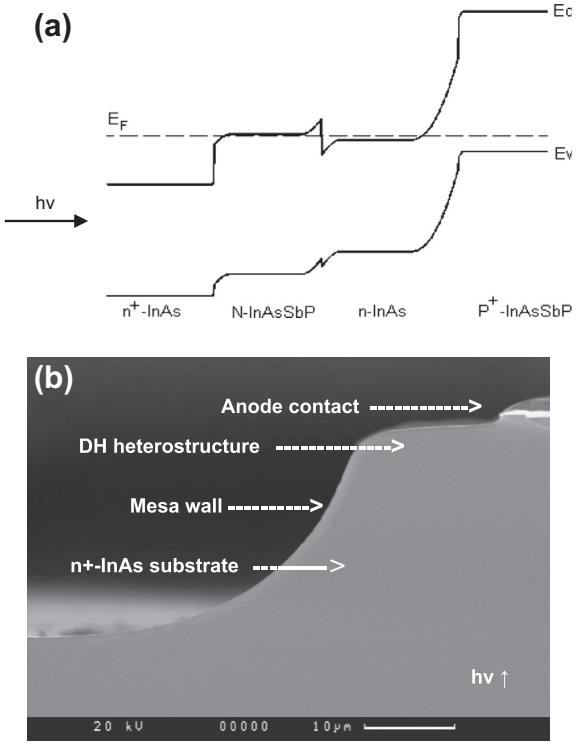


**Fig. 1.** (a) Schematic band diagram of the backside illuminated DH PD at zero bias [16]. (b) SEM image of the cleaved PD chip with mesa side wall. Part of the anode contact is seen in the right upper corner of the figure, while plane of the photo presents the $(1\bar{1}0)$ cleaved plane. Direction of nonequilibrium photon fluxes (hv) coming from Globar/Black Body are marked by the arrows on both (a) and (b) figures.

*I–V* characteristics were measured at $I = 10^{-12}$–$2 \times 10^{-3}$ A under the dark conditions at CW mode using the sub-femtoampere SourceMeter Keithley 6430 equipped with remote preamplifier; the responsivity was measured using Black Body model at 573 K while Globar was implemented in the spectral response measurements.

## 3. Results and discussion

### 3.1. Optical and photoelectrical characteristics

Fig. 2 presents relative PD spectral response $S_I$ at several temperatures in the 107–295 K range; uncorrected spectra contained distortions associated with $CO_2$ and water absorption around 2.6–2.7 μm wavelengths and thus for the sake of simplicity the distorted parts of the curves in Fig. 2 were substituted by the interpolated ones. As $n^+$-InAs substrate acts as a cut-off optical filter the short wave shoulder of the sensitivity spectrum depicted the substrate transmission in accordance with the backside illumination operation mode; peak responsivity value exhibited weak variation with temperature – feature previously observed in many InAs PDs [7,8,10,12,13].

P–n junction area being taken into account the room temperature peak responsivity in bare flip-chip DH PDs (that is, without Si lenses) amounted to 2.4 A/W which is slightly beyond the values published for InAs based detectors – apparently an assumption that the optical area ($A_o$) is the same as the p–n junction area ($A_e$) is not true in our case. Indeed the deep mesa etching process provides inclined mesa walls (see Fig. 1b) that contribute to the collection efficiency of photons and thus the simulated quantum efficiency at maximum $\eta$ based on the $A_o = A_e$ assumption exceeds unity. Stating the $\eta$ value as being equal to unity the optical area/p–n junction area ratio in our case is as high as $A_o/A_e = 1.3$; the latter value fits well the $A_o/A_e$ ratio for other flip-chip PDs (e.g. based on InAsSb) fabricated with similar to our deep mesa etching process and close physical dimensions.

### 3.2. Electrical characteristics

There have been no fully dark conditions in our experiments and thus in some cases the *I–V* characteristics did not cross the zero point in the *I–V* plane, e.g. we clearly observed shortcut positive PD current ranging from $3.7 \times 10^{-12}$ at 140 K to $1.0 \times 10^{-9}$ A at 190 K meaning that PD (active area) was exposed to unshielded

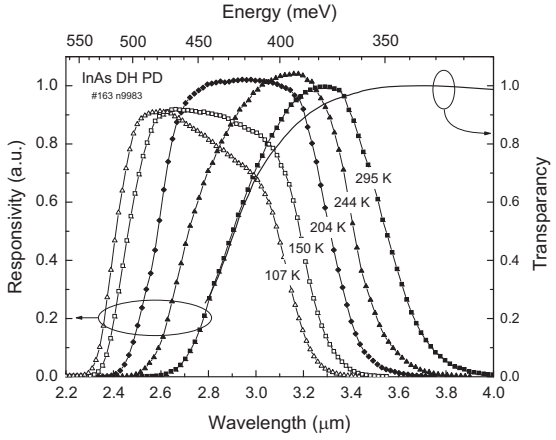


**Fig. 2.** Spectral response of the immersion lens DH PD at several temperatures (107, 150, 204, 244 and 295 K) and expected values of optical transparency of a 90 μm thick $n^+$-InAs substrate at 295 K. Presented temperature values refer to numbers that follow from superposition of the 50%-cut-off shift and temperature variation of the energy gap in n-InAs.

parts of our set-up that were colder than PD itself or in other words PD received and registered the so called "negative" optical beams. The above shortcut values were further used for current value corrections with the result that $I = 0$ at $V = 0$. The forward current exhibited step that divided two regions of exponential growth; step position was progressively changing from $U = 0.25$ V at 100 K down to 0.07 V at 190 K while room temperature $I$–$V$ characteristic was free of any peculiarities (steps). The above steps indicate leakage through p–n junction of some kind that saturates at high forward voltage; the leakage weakly depends on temperature with domination of the diffusion current at high temperatures.

As seen from left panel in Fig. 3 at $T < 100$ K and $0 > U > -2$ V the current was evidently below the set-up detection limit and we were thus unaware of real current values within the above range; starting from $-2$ V fast current growth (breakdown) took place, at temperatures higher than 160 K the above "breakdown" transformed into a leakage with weak dependence on $U$. Having in mind negligible influence of the leakage on current values at small reverse bias the saturation current values were determined as $I_o = I$ (at $U = -3kT/e$). These $I_o$ values together with saturation current and ideality factor values originated from the best fit of the forward current data and the $I = I_o(\exp(eU/\beta kT) - 1)$ expression are shown in Fig. 4.

As seen from plot in Fig. 4 the temperature dependence of the saturation current $I_o = B\exp(-E/kT)$ in both low and high current regions is characterized by a single activation energy value of $E = 0.35$ eV that is fairy close to the energy gap of the InAs active region and to activation energy reported recently for homo- [6] and heterojunction [12,13] InAs PDs. The proximity of the $E$ and $E_g$ values reflects domination of the diffusion current; this satisfactory agrees with the ideality factor value $\beta$ that was well below 1.5 in the whole 100–300 K temperature range.

### 3.3. Detectivity

For the sake of convenience when comparing with the published data we excluded sensitivity enhancement associated with collimation of radiation in our PDs and thus further considerations refer to "model" PD with non-reflective or/and shallow mesa side walls. Current sensitivity of the "model" PD was set 1.3 times smaller than the actual (measured) one. Fig. 5 presents superposition of data in Figs. 2 and 4 and the $R_o = \beta kT/I_o$, $D^*_{\lambda\max} = S_I(R_oA/4kT\Delta f)^{0.5}$ relations, where $I_o$ is the dark current, $\beta$ is the ideality factor, $k$ is

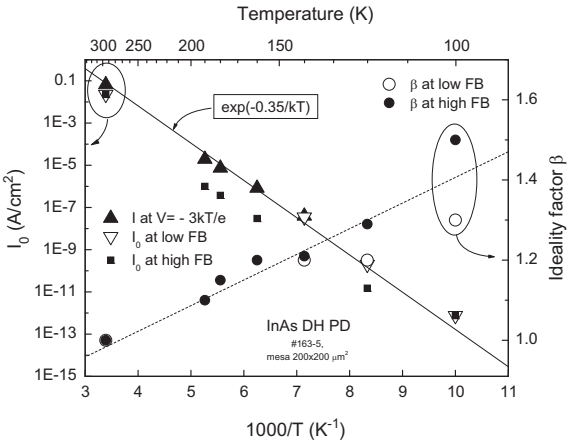


**Fig. 4.** Saturation current ($I_o$) and ideality factor ($\beta$) values derived from the reverse bias data (filled triangles up), at low (open triangles down and open circles) and high (filled triangles down and filled circles) forward current.

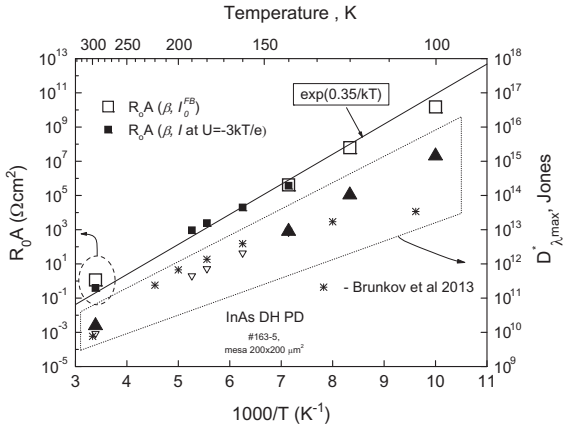


**Fig. 5.** $R_oA$ and $D^*_\lambda$ values vs. temperature in InAs DH PD. Open symbols refer to parameters extracted from the low current FB part of the $I$–$V$ characteristic while filled ones refer to current at $U = -3kT/e$. Stars present data for SH InAs PD from Ref. [13].

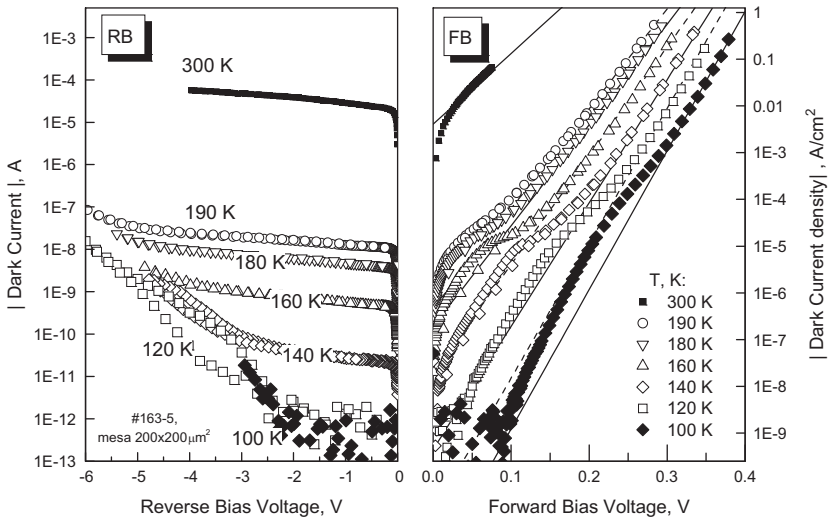


**Fig. 3.** $I$–$V$ characteristics in the 100–300 K temperature range. Lines on the right panel present exponential functions $I = I_o(\exp(eU/\beta kT) - 1)$ that fit high current $I$–$V$ parts where $\beta$ varies in the 1–1.5 range.

the Boltzmann constant, $T$ is the temperature, $S_I$ is the "modeled" current sensitivity, $A$ is the p–n junction area, $\Delta f = 1$ Hz. Fig. 5 shows also the $D^*_\lambda$ values previously reported for the SH InAs PDs in Ref. [13]. It follows from data in Fig. 5 that the detectivity $D^*_\lambda$ value grows by five orders when DH PD is cooled from 300 down to 100 K; at temperatures below 120 K $D^*_\lambda$ exceeds at least by an order of magnitude the corresponding values for the SH PD [6,12,13] obviously due to lower generation-recombination current/lower ideality factor in the DH PD. The above performance improvements may originate from better quality of the active layer and/or p–n junction or/and impact of the potential barriers at the n-InAsSbP/n-InAs heterojunction (the effect of the latter on zero bias resistance was already reported in [16]). At temperatures above 140 K the detectivity in both SH and DH PDs is of the same order, however the unlike SH in [12,13] the DH PDs exhibit mild reverse current growth at moderate bias voltage and thus suggest lower detection limit at reverse bias and more freedom for amplifier circuit design choice.

## 4. Conclusion

Introduction of an additional N-InAsSbP layer into a cooled P-InAsSbP/n-InAs heterostructure PD resulted in remarkable performance enhancement of radiation detection in the 3 μm spectral range due to lower saturation current and ideality factor values. Additional advantage of the DH PD over the traditional P-InAsSbP/n-InAs SH PD is lack of the reverse current breakdown at $|U| < 2$ V. BSI DH InAs PD demonstrated $D^*_\lambda$ ranging from $10^{15}$ at 100 K to $10^{13}$ cm Hz$^{1/2}$ W$^{-1}$ at 140 K; the latter value clearly indicates DH PD potential for creation detector systems operating at medium cooling conditions.

## References


[1] V.I. Stafeev, Mercury cadmium telluride: main semiconductor material of modern IR photoelectronics Proc. SPIE 4340, in: 16th International Conference on Photoelectronics and Night Vision Devices, November 28, 2000, p. 240. http://dx.doi.org/10.1117/12.407737.

[2] G.Yu. Sotnikova, S.E. Aleksandrov, G.A. Gavrilov, A3B5 photodiode sensors for low-temperature pyrometry, Proc. SPIE, vol. 8073, 80731A. http://dx.doi.org/10.1117/12.886309.

[3] G.Yu. Sotnikova, G.A. Gavrilov, S.E. Aleksandrov, A.A. Kapralov, S.A. Karandashev, B.A. Matveev, M.A. Remennyy, Low voltage $CO_2$-gas sensor based on III–V mid-IR immersion lens diode optopairs: where we are and how far we can go?, Sens J. IEEE 10 (2010) 225–234, http://dx.doi.org/10.1109/JSEN.2009.2033259.

[4] M.G. Mauk, V.M. Andreev, GaSb-related materials for TPV cells, Semicond. Sci. Technol. 18 (2003) S191–S201.

[5] V.A. Gevorkyan, V.M. Aroutiounian, K.M. Gambaryan, M.S. Kazaryan, K.J. Touryan, M.W. Wanlass, Liquid-phase electroepitaxial growth of low band-gap p-InAsPSb/n-InAs and p-InAsP/n-InAs diode heterostructures for thermophotovoltaic application, Thin Solid Films 451–452 (2004) 124–127.

[6] P.J. Ker, A.R.J. Marchall, J.P.R. David, C.H. Tan, Low noise high responsivity InAs electron avalanche photodiodes for infrared sensing, Phys. Status Solidi C9 (2012) 310–313, http://dx.doi.org/10.1002/pssb.201100277.

[7] X.Y. Gong, T. Yamaguchi, H. Kan, T. Makino, T. Iida, T. Kato, M. Aoyama, Y. Hayakawa, M. Kumagawa, Room temperature $InAs_xP_{1-x-y}Sb_y$/InAs photodetectors with high quantum efficiency, J. Appl. Phys. 36 (1997) 2614–2616.

[8] B.A. Matveev, N.V. Zotova, S.A. Karandashev, M.A. Remennyi, N.M. Stus', G.N. Talalakin, Backside illuminated In(Ga)As/InAsSbP DH photodiodes for methane sensing at 3.3 μm, Proc. SPIE 4650 (2002) 173–178.

[9] R.K. Lal, P. Chakrabarti, An analytical model of P-InAsSbP/$n^{0-}$InAs/$n^+$-InAs single heterojunction photodetector for 2.4–3.5 μm region, Opt. Quantum Electron. 36 (2004) 935–947.

[10] M.A. Remennyy, B.A. Matveev, N.V. Zotova, S.A. Karandashev, N.M. Stus, N.D. Ilinskaya, InAs and InAs(Sb)(P) (3–5 μm) immersion lens photodiodes for portable optic sensors, SPIE 6585 (2007), http://dx.doi.org/10.1117/12.722847. 658504 (1–8).

[11] M. Ahmetoglu (Afrailov), Photoelectrical characteristics of the InAsSbP based uncooled photodiodes for the spectral range 1.6–3.5 μm, Infrared Phys. Technol. 53 (2010) 29–32.

[12] N.D. Il'inskaya, S.A. Karandashev, N.M. Latnikova, A.A. Lavrov, B.A. Matveev, A.S. Petrov, M.A. Remennyi, E.N. Sevost'yanov, N.M. Stus', Cooled photodiodes based on a type-II single p-InAsSbP/n-InAs heterostructure, Tech. Phys. Lett. 39 (2013) 818–821.

[13] P.N. Brunkov, N.D. Il'inskaya, S.A. Karandashev, N.M. Latnikova, A.A. Lavrov, B.A. Matveev, A.S. Petrov, M.A. Remennyi, E.N. Sevostyanov, N.M. Stus', Single p-InAsSbP/n-InAs heterostructure PDs for operation in the 77–330 K range, in: Abstracts of the 12 Scientific-Technical Conference on Solid State Electronics, Smart functional radio and electronic apparatus, 24–25 October 2013, Moscow, pp. 152–156 (in Russian).;
P.N. Brunkov, N.D. Il'inskaya, S.A. Karandashev, N.M. Latnikova, A.A. Lavrov, B.A. Matveev, A.S. Petrov, M.A. Remennyi, E.N. Sevostyanov, N.M. Stus', P-InAsSbP/$n^o$-InAs/$n^+$-InAs photodiodes for operation at moderate cooling (150–220 K), Semiconductors (2014). in press.

[14] B. Matveev, N. Zotova, N. Il'inskaya, S. Karandashev, M. Remennyi, N. Stus', Spontaneous and stimulated emission in InAs LEDs with cavity formed by gold anode and semiconductor/air interface, Phys. Status Solidi (c) 2 (2) (2005) 927–930.

[15] P. Santhanam, D. Huang, R.J. Ram, M.A. Remennyi, B.A. Matveev, Room temperature thermo-electric pumping in mid-infrared light-emitting diodes, Appl. Phys. Lett. 103 (1 November) (2013) 183513, http://dx.doi.org/10.1063/1.4828566.

[16] B.A. Matveev, A.V. Ankudinov, N.V. Zotova, S.A. Karandashev, T.V. L'vova, M.A. Remennyy, A.Yu. Rybal'chenko, N.M. Stus', Properties of mid-IR diodes with n-InAsSbP/n-InAs interface, SPIE 7597 (2010), http://dx.doi.org/10.1117/12.841625. 75970G-(1–9).

[17] I. Vurgaftman, J.R. Meyer, L.R. Ram-Mohan, Band parameters for III–V compound semiconductors and their alloys, J. Appl. Phys. 89 (2001) 5815–5874.